Enhancing BCI System Performance through NDD Channel Configuration

Abdel fateh DOUDOU[1], Aicha REFFAD[1], Kamel MEBARKIA[2]

[1]LAS Laboratory, Electrotechnics Department, Faculty of Technology,
Setif 1 University, 19000 Setif, Algeria
[2]LIS Laboratory, Electronics Department, Faculty of Technology,
Setif 1 University, 19000 Setif, Algeria

E-mail: afdoudou19@gmail.com

Abstract - Motor Imagery Brain-Computer Interfaces (MI-BCIs) are artificial intelligence powered systems designed to detect brain activity patterns linked to the mental imagination and subsequently translate these patterns into instructions for controlling external devices. A hurdle in BCI motor imagery electroencephalography (MI-EEG) is the notable issue of achieving accurate recognition of imagined movements. In this paper, we present an innovative approach aimed to address the challenge of reducing the number of channels while concurrently introducing novel features. These features are grounded in the continuous wavelet transform and discrete wavelet transform (DWT), with the primary objective of enhancing the accuracy of the MI-EEG signals decoding. Our system leverages a comprehensive set of 220 features extracted from both the time and frequency domains. These features serve as input to a pre-trained SVM classifier, facilitating the precise identification of the respective movement classes, encompassing left/right hand, foot, and tongue. The proposed system's efficacy was assessed through the utilization of the BCI Competition IV Dataset 2a, with a focus on evaluating classification accuracy (CA). These results emphasize the superiority of the proposed method in achieving an impressive CA of 78.30%. Additionally, the approach significantly reduces the number of features selected by approximately 79%.

Keywords - brain–computer interface (BCI); electroencephalogram (EEG); motor imagery (MI); features extraction; SVM classifier; genetic algorithm.

I. INTRODUCTION

Brain-computer interfaces (BCIs) are considered pioneering assistive technologies, which play a transformative role in creating a direct connection between the human brain and external devices [1]. BCI technology grants individuals with disabilities the capability to communicate and engage them in their everyday activities autonomously [2], [3]. As a system, it possesses the capability to decipher specific brain signals, encompassing facets of our emotions and cognitive thoughts.

The brain's electrical activity is typically assessed through the use of an electroencephalogram (EEG), a straightforward and non-invasive technique that involves the placement of electrodes on the surface of the scalp to record and gather data regarding brain wave patterns [4]. EEG offers excellent temporal resolution, portability, low cost, and captures synchronous electrical signals generated by the brain. Nonetheless, the challenge with EEG signals in BCI systems lies in their non-stationary nature, low signal-to-noise ratio, and limited spatial resolution, necessitating the application of advanced signal processing techniques to cleanse the data from artifacts and extract relevant spatial, temporal, and frequency information for classification purposes [5]. Generally, five distinct categories of brain waves can be identified according to their frequency bands, each of these specific frequency ranges is linked to distinct mental states and cognitive activities: Delta waves, characterized by frequencies ranging from 0.5 to 4 Hz; Theta waves, with frequencies spanning from 4 to 8 Hz; Alpha waves, oscillating between 8 and 12 Hz; Beta waves, falling within the range of 12 to 30 Hz;

and finally, Gamma waves, with frequencies exceeding 30 Hz [5], [6].

Motor Imagery EEG (MI-EEG) represents a distinct category within non-invasive BCI methods. MI is a frequently utilized cognitive task where individuals are guided to mentally envision themselves carrying out a particular physical action, such as moving their right hand, left hand, foot, or tongue, without any actual physical execution [7]. Each specific cognitive task is associated with a unique class of MI. Deciphering this brain activity presents a difficulty within MI-EEG based BCI systems. The process of identifying MI-EEG data recorded from subjects encompasses several integral stages. These include initial preprocessing to prepare the data, extracting relevant features that capture essential information, selecting the most informative of these features, and finally, applying a classification model to distinguish and interpret the data effectively [8], [9]. Recently, machine learning techniques have demonstrated their dependability in accurately recognizing diverse Motor Imagery (MI) activities. For achieving successful classification of MI-EEG signals, it is imperative to have both an accurate and efficient feature extraction method, in conjunction with an effective classifier, as these components play pivotal roles in determining the overall effectiveness of the classification models.

Most contemporary MI-EEG predominantly leverages machine learning algorithms, making use of a wide array of classifier types, including but not limited to linear discriminant analysis (LDA), k-nearest neighbor (KNN), neural networks (NN), support vector machine (SVM), and logistic regression (LR), among others, for the classification of MI-EEG signals [10-15].

The primary objective of this work is to improve the performance of the BCI system by increasing the classification accuracy (CA) through the utilization of MI-EEG signal features. We have devised a system that focuses on the analysis of Beta-band oscillations in EEG signals, wherein we reduced 22 channels of EEG signals to 10 channels using a normal double difference (NDD) electrode configuration. We introduced a comprehensive set of 220 features obtained from both the time and frequency domains through the application of the discrete wavelet transform (DWT). These features were then employed as inputs for an SVM classifier to accurately identify Motor Imagery (MI) classes (left hand, right hand, foot, or tongue). The performance of the proposed method is evaluated using the BCI competition IV dataset 2a.

II. METHODOLOGY

A) MI-EEG Based BCI System

Deciphering the intention to initiate movement through the analysis of brain activity patterns represents a substantial challenge in the field of MI-EEG based BCI systems. Figure 1 provides a visual representation depicting the architecture of an MI-EEG based BCI system. This process involves several key steps, starting with preprocessing and feature extraction, followed by classification.

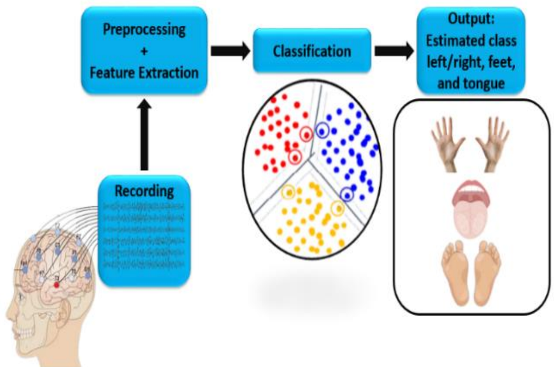

Fig. 1. A graphical depiction of an MI-EEG based BCI system.

The ultimate output of this process is the estimation of the class associated with the intended action, which could be left hand, right hand, feet, or tongue movement. These steps collectively enable individuals to communicate and control external devices using only their thoughts and imagination.

B) Description of the Dataset

To validate the proposed approach, a publicly accessible EEG dataset from BCI Competition IV is utilized as a means of verifying its viability and effectiveness. The dataset used is "dataset 2a" which contains EEG data gathered from 9 subjects [16]. Twenty-two electrodes were employed to record the EEG signals, as illustrated in Figure 2. For each subject, two separate sessions were recorded on different days. Each session is divided into 6 runs, with short breaks in between. A single run includes 48 trials, with 12 trials associated with each of the four possible classes, resulting in a total of 288 trials per session. During the experimental setup, the subjects were seated comfortably in an armchair positioned in front of a computer screen. Each trial began with a fixation cross and an auditory alert at t = 0 s. After 2 seconds, a cue in the form of an arrow pointing left, right, down, or up, corresponding to the four classes (left hand, right hand, foot, or tongue), appeared for 1.25 s. Subjects performed motor imagery tasks until the fixation cross vanished at 6 s, followed by a short break, and the screen returned to black.

This experimental paradigm is visualized in Figure 3. The signals were sampled at a rate of 250 Hz and subjected to bandpass filtering between 0.5 Hz and 100 Hz, along with the incorporation of a 50 Hz notch filter.

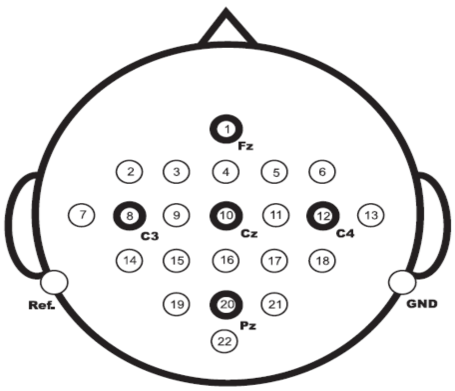

Fig. 2. The electrode placement follows the international 10-20 system.

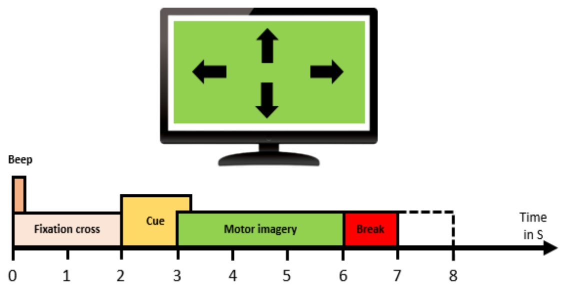

Fig. 3. Experimental paradigm of the BCI Competition IV Dataset 2a.

C) Normal double difference (NDD)

The normal double difference (NDD) configuration reduces the number of channels by combining or summarizing information from multiple channels into a smaller set of channels [17]. This reduction is achieved by taking the difference between pairs of neighboring channels [18]. NDD effectively preserves important information while minimizing redundancy, resulting in a more streamlined and computationally efficient channel configuration.

In this dataset, the NDD technique effectively reduces the number of channels from 22 to 10. Figure 4 depicts the arrangement of these 22 electrodes along with the 10 channels (electrodes 4, 8, 9, 10, 11, 12, 15, 16, 17, and 20) utilized to obtain the corresponding 10 NDD signals.

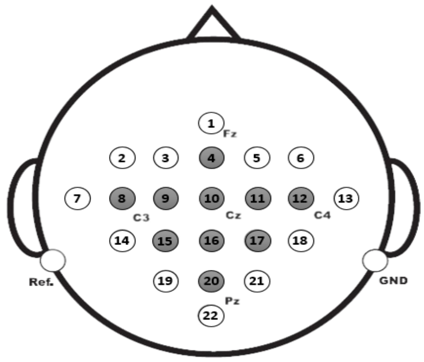

Fig. 4. Configuration of 22 electrodes enabling the acquisition of 10 NDD-type signals.

Equation (1) provides a mathematical representation of the first NDD process. C_1 represents channel 1.

$$NDD_1 = 4 * C_4 - (C_1 + C_3 + C_{10} + C_5) \tag{1}$$

This approach streamlines the data, making it more computationally efficient and optimizing the channel configuration without sacrificing important information for analysis.

D) Feature extraction

To extract valuable motor imagery (MI) information from its EEG signals, preprocessing is typically conducted while signal frequency filtering serves as a common preliminary step in the majority of studies. This is done for two primary reasons: to identify the most pertinent frequency bands for MI tasks and to eliminate any artifacts that may be present in the signals. Initially, we employ a second-order Butterworth band-pass filter to process all 10 NDD signals within the designated frequency range of [13-30] Hz. In the analysis of Motor Imagery EEG (MI-EEG), feature extraction assumes a pivotal role, as it serves to convert intricate EEG signals into useful data. The features obtained through extraction capture the critical patterns and attributes linked to the imagined brain tasks. The selection of the appropriate features is of utmost significance, as it greatly impacts the effectiveness of the CA.

Various techniques, including the common spatial patterns (CSP) [19], Fourier transform (FT) [20], power spectral density (PSD) [21], and wavelet transform (WT) [4], [9], can be applied to analyze EEG signals. In this work, to effectively distinguish between classes, we utilize a range of features that encompass both the time domain and the time-frequency domain, incorporating methods such as continuous wavelet transform (CWT) and discrete wavelet transform (DWT). Features are derived from the 10 NDD signals.

The following section outlines the statistical operators, continuous wavelet transform (CWT), and discrete wavelet transform (DWT) applied in the computation of the proposed features.

Wavelet transform (WT) is typically classified into two categories: CWT and DWT. To address the issue of resolution limitations in short-time Fourier transform, CWT employs wavelets that are continuously adapted and transformed. However, because the wavelets used in CWT are non-orthogonal, it results in redundant representations of signals. On the other hand, DWT shares similarities with CWT but, to eliminate redundancy, employs wavelets that have been discretely adjusted and altered.

The CWT Equation :

$$C_x(a,b) = \frac{1}{a}\int_{-\infty}^{\infty} x(t)\Psi\left(\frac{t-b}{a}\right)dt \tag{2}$$

In this equation, 'a' represents the scale parameter, while 'b' denotes the parameter for the temporal position of the mother wavelet Ψ.

The DWT Equation:

$$A[k] = \sum_n x[n].g[2k-n] \tag{3}$$

$$D[k] = \sum_n x[n].h[2k-n] \tag{4}$$

'$x[n]$' signifies the signal, '$A[k]$' and '$D[k]$' represent the approximation and detailed coefficients, respectively. The DWT was subjected to a three-level decomposition using the sym2 wavelet function.

Variance (*var*) serves as a valuable indicator of signal power and can be defined as:

$$\boldsymbol{var} = \frac{1}{N-1}\sum_{i=1}^{N}(x_i)^2 \tag{1}$$

Here, 'x' represents the signal, and 'N' is the length of the signal.

Mean Curve Length (*MCL*) quantifies signal complexity and irregularity, as expressed in equation (6)

$$\boldsymbol{MCL} = \frac{1}{N}\sum_{i=2}^{N}|x_i - x_{i-1}| \tag{6}$$

The '*log*' detector (LD) for EEG is a signal processing technique that transforms EEG data into a logarithmic scale, enhancing the visibility of subtle variations in electrical brain activity as defined by the equation (7).

$$\boldsymbol{LD} = exp(\frac{1}{N}\sum_{i=1}^{N} log(|x_i|)) \tag{7}$$

Kurtosis and skewness are statistical measures that provide valuable insights into the shape and distribution of EEG signal data, aiding in the characterization of its frequency content and symmetry, as expressed by equations 8 and 9.

$$\boldsymbol{kurtosis} = \frac{1}{N\sigma^2}\sum_{i=1}^{N}(x_n - \mu)^4 \tag{8}$$

$$\boldsymbol{skewness} = \frac{1}{N\sigma^3}\sum_{i=1}^{N}(x_n - \mu)^3 \tag{9}$$

Here, μ represents the mean, and σ signifies the standard deviation of the signal.

Root Mean Square (RMS) is a statistical measure widely used in EEG signal analysis to quantify the signal's amplitude and overall energy. RMS is calculated using the formula:

$$\boldsymbol{RMS} = \sqrt{\frac{1}{N}\sum_{i=1}^{N}(x_i)^2} \tag{10}$$

Mean Absolute Deviation (MAD) and Standard Deviation (STD) are statistical measures employed in EEG signal analysis to assess signal variability and dispersion and are expressed by the following formulas :

$$\boldsymbol{mad} = \frac{1}{N}\sum_{n=1}^{N}|x_n - \mu| \quad (11)$$

$$\boldsymbol{rms} = \sqrt{\frac{1}{N}\sum_{i=1}^{N}(x_i - \mu)^2} \quad (12)$$

Where μ represents the mean of the data set. Table 1 presents a detailed compilation of the 220 proposed features along with their respective mathematical formulas.

Table 1. Proposed Features and Their Formulations.

features	mathematical formulas
f_n	$sum(cw_i(i1+1)^2)$ i =1..10 ; $i1$=1..4 ; n =1…40
f_n	$sqrt(f1_{n-40}/f1_{(n-40)+4})$ n =41…44
f_n	$sqrt(f1_{(n-44)+8}/f1_{(n-44)+12})$ n =45…48
f_n	$sqrt(f1_{(n-48)+16}/f1_{(n-48)+20})$ n =49…52
f_n	$sqrt(f1_{(n-52)+24}/f1_{(n-52)+28})$ n =53…56
f_n	$sqrt(f1_{(n-56)+32}/f1_{(n-56)+36})$ n =57…60
f_n	$sum(NDD_i{}^2)$ n =61…70
f_n	f_{n1}/f_{n1+1} $n1 = 61, 63, 65, 67, 69$; n =71…75
f_n	$mad(NDD_i)$ n =76…85
f_n	f_{n2}/f_{n2+1} $n2 = 76, 78, 80, 82, 84$ n =86…90
f_n	$var(NDD_i)$ n =91…100
f_n	f_{n3}/f_{n3+1} $n3 = 91, 93, 95, 97, 99$ n =101…105
f_n	$MCL(NDD_i)$ n =106…115
f_n	f_{n4}/f_{n4+1} $n4 = 106, 108, 110, 112, 114$ n =116…120
f_n	$skewness(NDD_i)$ n =121…130
f_n	f_{n5}/f_{n5+1} $n5 = 121, 123, 125, 127, 129$ n =131…135
f_n	$std(NDD_i)$ n =136…145
f_n	f_{n6}/f_{n6+1} $n6 = 136, 138, 140, 142, 144$ n =146…150
f_n	f_t/f_{t+15} $t = 121 \dots 130$ n =151…160
f_n	$kurtosis(NDD_i)$ n =161…170
f_n	f_{n7}/f_{n7+1} $n7 = 161, 163, 165, 167, 169$ n =171…175
f_n	$rms(NDD_i)$ n =176…185
f_n	f_{n8}/f_{n8+1} $n6 = 176, 178, 180, 182, 184$ n =186…190
f_n	$LD(NDD_i)$ n =191…200
f_n	f_{n9}/f_{n9+1} $n6 = 191, 193, 195, 197, 199$ n =201…205
f_n	$sum(A_{t3}{}^2/A_{t3+1}{}^2)$ $t3 = 1, 3, 5, 7, 9$ n =206…210
f_n	$mean(abs(A_{t3}/A_{t3+1}))$ n =211…215
f_n	$rms(abs(A_{t3}/A_{t3+1}))$ n =216…220

E) Machine Learning Algorithm

Following the feature extraction process, the MI-EEG signals feature set is constructed. This feature set feeds a linear SVM classifier. The SVM is a machine learning algorithm that classifies data by finding an optimal linear boundary, or hyperplane, to separate different classes. It maximizes the margin between data points, enhancing generalization and robustness.

III. RESULTS

To evaluate the suitability of the proposed method, we conducted experiments using BCI Competition IV Dataset 2a. In practice, subjects are unable to perform MI tasks at identical initial time positions and durations. To address this issue, we employed firefly optimization to determine the optimal initial time position and processing duration for each individual subject, while leveraging the 220 proposed features, thereby empowering the linear SVM classifier to enhance. The final results were evaluated through the application of ten-fold cross-validation. Table 2 shows the CA using the proposed features, optimized with the best initial time position and processing duration using a linear SVM classifier.

Table 2. CA of the proposed features with the best initial time position and processing duration.

Subjects	initial time position (s)	processing duration (s)	CA %
S1	2.62	2.93	73.79
S2	2.59	3.34	62.36
S3	2.7	2.79	81.64
S4	2.59	2.70	45.5
S5	2.95	2.16	46.64
S6	2.59	0.73	56
S7	2.59	2.61	79.5
S8	2.52	2.81	78.36
S9	2.59	0.65	86.71

In the pursuit of improving CA, Genetic Algorithms (GA) were employed to fine-tune and optimize the SVM classifier individually for each subject. GA is a class of optimization and search algorithms inspired by the process of natural selection and evolution [22]. They serve as powerful computational tools for solving complex problems by mimicking the principles of genetic variation, selection, and reproduction. In this study, GA optimization was applied to choose the most appropriate features and reduce redundant features, with the primary objective of improving CA. Figure 5 illustrates the Genetic Algorithm (GA) optimization process, showcasing the selection of relevant features for the subject with the highest CA and the subject with the lowest CA.

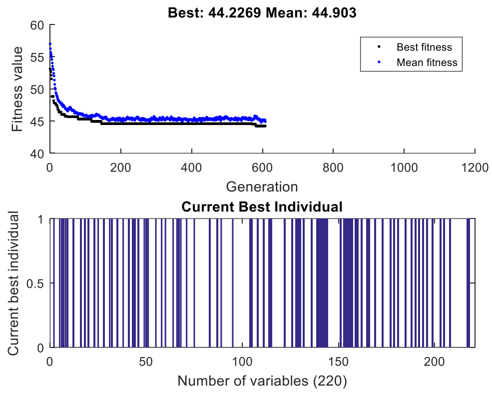

(a)

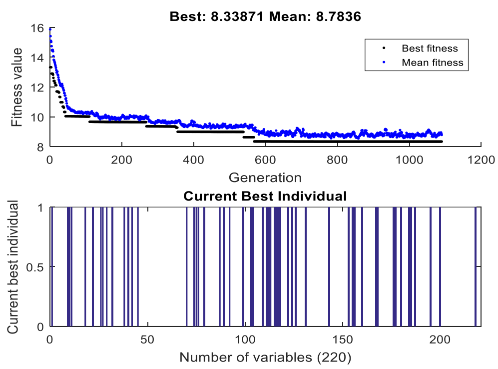

(b)

Fig. 5. Feature Selection with GA. "(a) Relevant Features for Subject 4 and (b) Relevant Features for Subject 9

The GA optimization process explores the best combination among an astonishing 2^{220} possibilities. In contrast to the enormous number of 2^{220} potential feature sets, the feature set chosen by GA stands out in its ability to effectively differentiate Motor Imagery EEG (MI-EEG), ultimately resulting in improved classification performance. Table 3 presents the CA results following the feature selection process.

The outcome highlights that, in conjunction with the SVM classifier and GA optimization, the classifier attained an average CA of 78.30%, and reduced the number of selected features (SF) by approximately 77% of the entire number of features (220).

Table 3. CA after features selection.

Subjects	SF	CA %
S1	49	87.07
S2	44	75.93
S3	37	89.71
S4	84	55.78
S5	93	65.43
S6	55	70.07
S7	51	90.36
S8	37	87.72
S9	53	91.67
Mean		78.30

Additionally, it is noteworthy that subject 4 achieved a CA of 55.78% while subject 9 yielded 91.67%. In light of this, we conducted an in-depth analysis by visually examining the maps of bioelectric signals, specifically focusing on the 10-channel NDD configuration. This analysis contributed valuable insights into the precise localization and spatial distribution of electrical activity, particularly in the context of MI. This examination allowed us to determine if the electrical activity associated with the MI class was accurately positioned and adequately represented in our EEG data specifically in the right place of the scalp. Figure 6 provides a visual representation of the bioelectric signals from the activated brain regions associated with various motor imagery tasks performed by Subjects 4 and 9, including left hand, right hand, foot, and tongue movements.

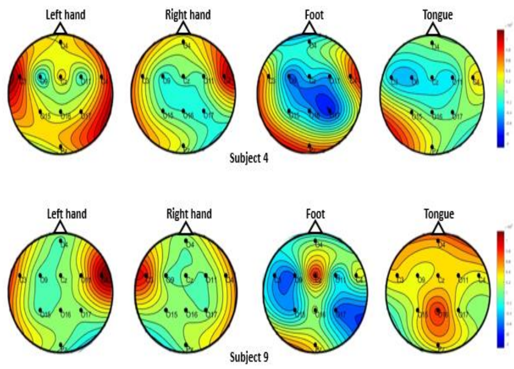

Fig. 6. Activated brain regions during Motor Imagery Tasks (left hand, right hand, foot, and tongue movements) in Subjects 4 and 9.

These illustrations show the RMS values (as indicated by the color scale) of differential voltage detected across the 10 NDD channels, where red areas signify an elevation in activity, while blue areas indicate a reduction. In Figure 6, it is evident that the electrical activity related to the MI class in the case of subject 4 is localized in incorrect regions, while for subject 9, the electrical activity associated with the MI class is correctly situated in the intended regions. The difference in accuracy between subject 4 and subject 9 can be attributed to the inaccurately localized electrical activity linked to the MI class, which, in turn, is associated with the subjects' accurate execution of the motor imagery task.

Next, we will evaluate our proposed approach to determine how well it performs in comparison to previously established methods. Table IV presents a performance comparison between our method and previous approaches in terms of MI-EEG CA using the same dataset (BCI Competition IV Dataset 2a). This evaluation focuses on the differentiation of motor movements involving the left/right hand, tongue, and foot through the utilization of MI-EEG signals. These studies employed a range of feature extraction techniques and classifiers in their research. Notably, as shown in Table 4, it becomes evident that the specific subset of features chosen from the initial set of 220 proposed features, in conjunction with SVM, resulted in a substantial enhancement of CA, reaching an impressive 78.30%.

Table 4. CA Comparative Analysis of Classification Accuracy (CA) with Previous Studies.

	works	methods	Acc(%)
Dataset	K.K. Ang, et al [23].	FBCSP	67.42
	Dong et al [24].	PSCSP	74.39
	Amin et al [25].	MCNN	75.72
	Our work	**NDD with 220 features**	**78.30**

IV. CONCLUSION

The performance of a BCI system is contingent on the choice of features and classifiers used for decoding brain-related tasks. Using the NDD method to reduce the number of channels from 22 to 10 channels is significant for the BCI system. In this paper, we propose 220 features that were input to linear SVM.

Moreover, we further improved this accuracy by employing GA optimization to pinpoint the most informative feature set for the linear SVM classifier. Following a comprehensive evaluation of our approach using the publicly available BCI competition database, we attained an impressive peak accuracy of 78.30% on the BCI Competition IV Dataset 2a. These results validate that the proposed approach outperforms existing methods in terms of CA, all while significantly reducing computational complexity through an approximate 79% reduction in the number of features.

V. ACKNOWLEDGMENTS

The authors would like to acknowledge the Institute for Knowledge Discovery (Laboratory of Brain-Computer Interfaces), Graz University of Technology, for providing the dataset online. (https://www.bbci.de/competition/iv).

VI. REFERENCES

[1] R. Rajan and S. Devassy, Improving Classification Performance by Combining Feature Vectors with a Boosting Approach for Brain Computer Interface (BCI), in *Book/Conference Title*, pp. 73-85, 2017.

[2] P. Xu, P. Yang, X. Lei, and D. Yao, An Enhanced Probabilistic LDA for Multi-Class Brain Computer Interface, *PLoS ONE*, vol. 6, p. e14634, 2011.

[3] M.K. Chowdary, J. Anitha, and D.J. Hemanth, Emotion Recognition from EEG Signals Using Recurrent Neural Networks, *Electronics*, vol. 11, p. 2387, 2022.

[4] K. Mebarkia and A. Reffad, Multi optimized SVM classifiers for motor imagery left and right hand movement identification, *Australas. Phys. Eng. Sci. Med.*, vol. 42, no. 4, pp. 949-958, August 2019.

[5] S. Vaid, P. Singh, and C. Kaur, EEG signal analysis for BCI interface: A review, in *2015 Fifth International Conference on Advanced Computing & Communication Technologies*, pp. 143-147, IEEE, February 2015.

[6] E. Rossi, S. Pereira Soares, Y. Prystauka, M. Nakamura, and J. Rothman, Riding the (brain) waves! Using neural oscillations to inform bilingualism research, *Bilingualism: Language and Cognition*, vol. 26, no. 1, pp. 202-215, 2023.

[7] P. Gaur, R. B. Pachori, H. Wang, and G. Prasad, A Multi-class EEG-based BCI Classification Using Multivariate Empirical Mode Decomposition-Based Filtering and Riemannian Geometry, *Expert Systems with Applications*, vol. 95, pp. 201-211, 2018.

[8] Y. Ming, W. Ding, D. Pelusi, D. Wu, Y.-K. Wang, M. Prasad, and C.-T. Lin, Subject Adaptation Network for EEG Data Analysis, *Appl. Soft Comput.*, vol. 84, p. 105689, 2019.

[9] A. Reffad and K. Mebarkia, Motor Imagery Hand Movements Recognition Using SVM Classifier and Genetic Algorithm Optimization, in *19th International Multi-Conference on Systems, Signals & Devices (SSD)*, Sétif, Algeria, 2022, pp. 1125-1129.

[10] G. Roy and S. Bhaumik, Classification of MI EEG Signal Using Minimum Set of Channels to Control a Lower Limb Assistive Device, *J. Inst. Eng. India Ser. B*, 2022.

[11] S. M. Imran, M. T. F. Talukdar, S. K. Sakib, N. S. Pathan, and S. A. Fattah, Motor Imagery EEG Signal Classification Scheme Based on Wavelet Domain Statistical Features, *2014 International Conference on Electrical Engineering and Information & Communication Technology*, Dhaka, Bangladesh, 2014.

[12] S. Siuly and Y. Li, Improving the Separability of Motor Imagery EEG Signals Using a Cross Correlation-Based Least Square Support Vector Machine for Brain–Computer Interface, in *IEEE Transactions on Neural Systems and Rehabilitation Engineering*, vol. 20, no. 4, pp. 526-538, July 2012.

[13] J. Luo, X. Gao, X. Zhu, B. Wang, N. Lu, and J. Wang, Motor Imagery EEG Classification Based on Ensemble Support Vector Learning, *Computer Methods and Programs in Biomedicine*, vol. 193, 2020, 105464. ISSN 0169-2607.

[14] RA Khan, N. Rashid, M. Shahzaib, UF. Malik, A. Arif, J. Iqbal, et al., A Novel Framework for Classification of Two-Class Motor Imagery EEG Signals Using Logistic Regression Classification Algorithm, *PLoS ONE*, vol. 18, no. 9, p. e0276133, 2023.

[15] S. Siuly, Y. Li, and Y. Zhang, Cross-Correlation Aided Logistic Regression Model for the Identification of Motor Imagery EEG Signals in BCI Applications, in *EEG Signal Analysis and Classification*, Health Information Science, Springer, Cham, 2016.

[16] C. Brunner, R. Leeb, G. Müller-Putz, et al., BCI Competition 2008–Graz Data Set A, *Inst. Knowledge Discovery (Laboratory of Brain-Computer Interfaces), Graz University of Technology*, vol. 16, 2008, pp. 1-6.

[17] D. J. McFarland, L. M. McCane, S. V. David, and J. R. Wolpaw, Spatial Filter Selection for EEG-Based Communication, *Electroencephalography and Clinical Neurophysiology*, vol. 103, no. 3, pp. 386-394, 1997. ISSN 0013-4694.

[18] Y. Li, K. Ang, and C. Guan, Digital Signal Processing and Machine Learning, in *Digital Signal Processing and Machine Learning*, 2011, pp. 305-330.

[19] C. Liu, H.-B. Zhao, C.-S. Li, and H. Wang, CSP/SVM-based EEG classification of imagined hand movements, *Dongbei Daxue Xuebao/Journal Northeast. Univ.*, vol. 31, no. 8, pp. 1098-1101, 2010.

[20] D. Coyle, G. Prasad, and T. M. McGinnity, A time-frequency approach to feature extraction for a brain-computer interface with a comparative analysis of performance measures, *EURASIP Journal on Applied Signal Processing*, vol. 2005, no. 19, pp. 3141-3151, Dec. 2005.

[21] C. Chao, D. Shin, A. N. Belkacem, and C. Wang, EEG-Based Anxious States Classification Using Affective BCI-Based Closed Neurofeedback System, *Journal of Medical and Biological Engineering*, vol. 41, no. 1, pp. 98-108, Feb. 2021.

[22] H. Li, Y. Hu, Y. Li, and D. Li, Channel Selection by Rayleigh Coefficient Maximization Based Genetic Algorithm for Classifying Single-Trial Motor Imagery EEG, Neurocomputing, vol. 121, pp. 423-433, 2013.

[23] K.K. Ang et al., Filter bank common spatial pattern algorithm on BCI Competition IV datasets 2a and 2b," Front. Neurosci., vol. 6, p. 39, 2012.

[24] E. Dong et al., "A novel hybrid kernel function relevance vector machine for multitask motor imagery EEG classification," Biomed. Signal Process. Control, vol. 60, 2020, 101991.

[25] S.U. Amin et al., "Deep learning for EEG motor imagery classification based on multi-layer CNNs feature fusion," Futur. Gener. Comput. Syst., vol. 101, 2019, pp. 542-554.